Accelerated Publications

Structure and Mechanism of Peptide Methionine Sulfoxide Reductase, an "Anti-Oxidation" Enzyme[†,‡]

W. Todd Lowther,[§] Nathan Brot,[||] Herbert Weissbach,[⊥] and Brian W. Matthews*[,§]

Institute of Molecular Biology, Howard Hughes Medical Institute and Department of Physics, University of Oregon, Eugene, Oregon 97403, Hospital for Special Surgery, Weill Medical College of Cornell University, New York, New York 10021, and Center for Molecular Biology and Biotechnology, Florida Atlantic University, Boca Raton, Florida 33431

Received August 25, 2000

ABSTRACT: Peptide methionine sulfoxide reductase (MsrA) reverses oxidative damage to both free methionine and methionine within proteins. As such, it helps protect the host organism against stochastic damage that can contribute to cell death. The structure of bovine MsrA has been determined in two different modifications, both of which provide different insights into the biology of the protein. There are three cysteine residues located in the vicinity of the active site. Conformational changes in a glycine-rich C-terminal tail appear to allow all three thiols to come together and to participate in catalysis. The structures support a unique, thiol−disulfide exchange mechanism that relies upon an essential cysteine as a nucleophile and additional conserved residues that interact with the oxygen atom of the sulfoxide moiety.

Biological aging is thought to be a consequence of numerous factors, some under genetic control and others more stochastic in nature, particularly random cell damage via reactive oxygen species generated from normal and pathological processes (*1*, *2*). The oxidation of methionine to methionine sulfoxide, Met(O),[1] has been implicated in a variety of neurodegenerative diseases, emphysema, cataractogenesis, and rheumatoid arthritis (reviewed in refs *1*−*4*). At the same time, the readily oxidizable nature of surface methionines suggests that these may act as an endogenous oxidant defense system (*5*). Other studies indicate that Met oxidation and/or reduction is involved in regulating potassium channel function and other cellular signaling mechanisms (*3*, *6*, *7*).

The reduction of Met(O) to Met, both as the free amino acid and when incorporated into proteins, is mediated by peptide methionine sulfoxide reductase (MsrA, EC 1.8.4.6). This enzyme is a member of the minimal gene set required for life (*8*) and is found in all mammalian tissues, with the highest levels in the cerebellum and kidney (*9*, *10*). The sequences of the presumed catalytic domains of the MsrAs are highly conserved [e.g., human, *Escherichia coli*, and yeast MsrAs are 88, 60, and 34% identical to bovine MsrA (bMsrA), respectively] (*11*, *12*). MsrA has the ability to provide protection against oxidative stress in vivo (*13*, *14*). It also appears to be involved in the attachment of pathogenic microorganisms to eukaryotic and plant cells (*15*−*17*) and in the onset of Alzheimer's disease (*18*).

The reduction of Met(O) and other small aliphatic sulfoxides by MsrA is stereospecific and is independent of protein-bound metals or cofactors (*11*, *12*, *19*, *20*). The requirement for a Cys-mediated electron donor (i.e., dithiothreitol in vitro or a thioredoxin-regeneration system in vivo), however, suggested the involvement of one or more Cys residues in catalysis (*11*, *21*). MsrAs contain within their presumed active sites a conserved Gly-Cys-Phe-Trp-Gly motif (*12*, *19*). Mutation of the Cys residue in either bovine or yeast MsrA results in a complete loss of activity (*12*, *19*). Catalysis is presumed to occur through a series of thiol−disulfide exchange steps (*12*), although an alternative mechanism utilizing a sulfenic acid intermediate has been proposed (*19*).

In this report, we present the structures of two modifications of bMsrA. The first structure is a complex with DTT and was determined to 1.6 Å resolution by multiwavelength anomalous dispersion (MAD) (Table 1). The second modification includes an additional 10 residues at the C-terminus and was determined by molecular replacement to 1.7 Å resolution (Table 1). Taken together, the two structures identify the catalytic residues, suggest a plausible mechanism of action, and illustrate the presumed modes of interaction of the enzyme with both DTT and thioredoxin.

[†] This work was supported in part by grants from the National Institutes of Health (Grant F32-GM17536 to W.T.L. and Grant GM20066 to B.W.M.) and Hoffmann-La Roche.

[‡] The coordinates have been deposited with the Protein Data Bank as entries 1FVA and 1FVG.

* To whom correspondence should be addressed. E-mail: brian@uoxray.uoregon.edu. Phone: (541) 346-2572. Fax: (541) 346-5870.

[§] University of Oregon.

[||] Weill Medical College of Cornell University.

[⊥] Florida Atlantic University.

[1] Abbreviations: bMsrA, bovine peptide methionine sulfoxide reductase; CT-1 and CT-2, crystal variants 1 and 2, respectively; DMSO, dimethyl sulfoxide; DTT, dithiothreitol; EDTA, ethylenediaminetetraacetic acid; MAD, multiwavelength anomalous dispersion; Met(O), methionine sulfoxide.

10.1021/bi0020269 CCC: $19.00
Published on Web 10/13/2000

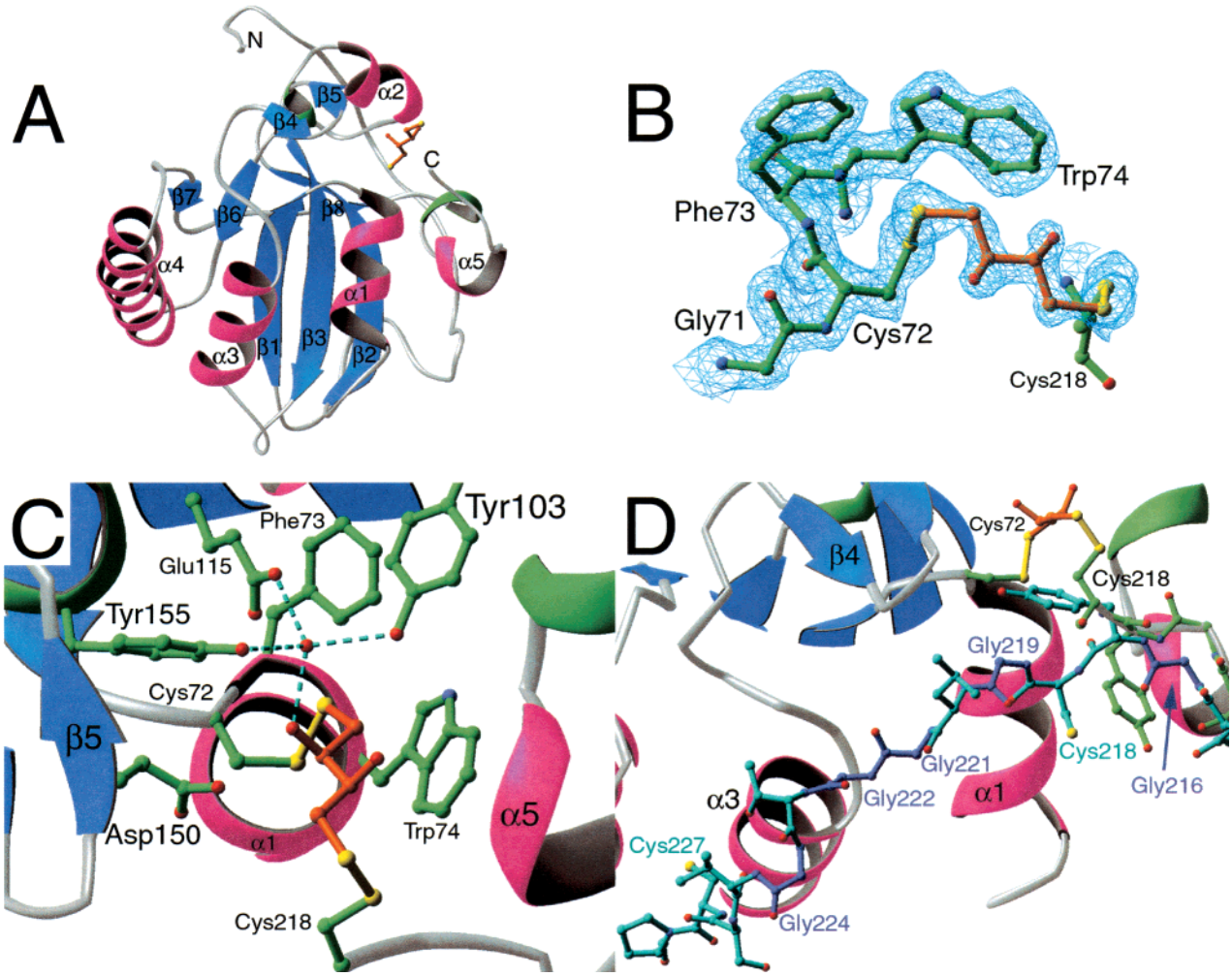

FIGURE 1: Topological features of MsrA. (A) Overall fold of the CT-1 form of bMsrA in complex with DTT (orange carbon atoms) generated with RIBBONS (*30*). The α-helices (magenta) and *β*-strands (light blue) are numbered consecutively on the basis of the primary sequence. The 3-10-helices are colored green. Atom colors are as follows: nitrogen, blue; oxygen, red; and sulfur, yellow. (B) MAD-phased, experimental electron density map contoured at 1σ surrounding the signature Gly^{71}-Cys-Phe-Trp-Gly^{75} motif (green carbon atoms) and the covalent DTT complex in the active site. (C) Molecular interactions between enzyme, solvent, and DTT. Five secondary structure elements (α1, α2, *β*3, *β*5, and one 3-10-helix) contribute conserved residues that interact (indicated by dashed, cyan bonds) with DTT via solvent-mediated hydrogen bonds (Tyr^{103}, Glu^{115}, and Tyr^{155}), a disulfide bond to the catalytically essential Cys^{72}, and hydrophobic interactions (Phe^{73} and Trp^{74}). Cys^{218}, located in the glycine-rich C-terminal tail, also formed a disulfide linkage with the opposite end of the DTT molecule. (D) The extended glycine-rich, C-terminal tail of the CT-2 crystal structure is shown in blue and cyan extending from the top right to the bottom left. The much shorter C-terminus of the CT-1 structure, which ends at residue 219, is shown in green with the DTT adduct in yellow and orange. The overall structures of CT-1 and CT-2 are very similar with root-mean-square discrepancy between α-carbon atoms of 0.62 Å (residues 30−218). The secondary structure elements that are shown are for CT-1.

MATERIALS AND METHODS

The mass spectrometric analysis of bMsrA fragments produced by chymotrypsin treatment led to the identification of two different truncation variants of bMsrA that would crystallize, CT-1 (residues 21−219) and CT-2 (residues 13−229). The two variants were obtained by the addition of stop codons to the 3′-end of the original *E. coli* overexpression construct [residues 1−233 (*12*)] and the removal of the N-terminal His tag by varying degrees of digestion with chymotrypsin.

Crystals of CT-1 containing seleno-Met (*22*) were obtained by the vapor diffusion method by mixing equal volumes of protein [12 mg/mL, 30 mM DTT, 16 mM Hepes (pH 7.4), 16 mM NaCl, 0.08 mM EDTA, and 6% DMSO] and well solution [100 mM citrate/Na_2HPO_4 (pH 4.75) 26−31% PEG 8000] at room temperature. Crystals of CT-2 without seleno-Met were grown in a similar manner at 4 °C with 5% 1,4-butanediol instead of DMSO in the protein buffer and the addition of 100 mM NaCl to the well solution (21−25% PEG 8000). CT-1 crystals exhibited *C*2 symmetry (a = 45.8 Å, b = 76.9 Å, c = 56.8 Å, β = 109.2°, one molecule/asymmetric unit), while those of the CT-2 were of space group $P2_1$ (a = 53.7 Å, b = 66.2 Å, c = 62.1 Å, β = 91.0°, two molecules/asymmetric unit).

Data for crystals cryoprotected in paratone were collected at 100 K with the CCD detector on beamline 9-2 at the Stanford Synchrotron Radiation Laboratory. Data were merged and scaled (Table 1) using DENZO and SCALEPACK (*23*). Three of four potential selenium sites were identified by SOLVE (*24*). MAD phases were refined using SHARP (*25*) and improved by solvent flattening with SOLOMON (*26*). The experimental electron density for residues 27−218 (Figure 1B) was readily traceable despite weak density

Table 1: Crystallographic Data, Phasing, and Refinement[a]

Crystallographic Data							
data set	λ (Å)	d_{min} (Å)	no. of observed reflections	no. of unique reflections	completeness (%)	$\langle I\rangle/\langle\sigma(I)\rangle$	R_{merge} (%)
seleno-Met CT-1							
anomalous peak (λ1)	0.9787	1.6	85832	23472	95.8 (93.9)	37.2 (8.0)	3.8 (17.1)
inflection point (λ2)	0.9788	1.6	95460	23729	96.3 (93.8)	40.1 (8.6)	3.4 (14.8)
high-energy remote (λ3)	0.9537	1.6	95293	23646	96.6 (94.6)	42.1 (9.4)	3.4 (13.7)
native CT-2	1.000	1.7	157688	46997	97.7 (84.0)	35.7 (3.5)	3.4 (22.4)

Phasing			
overall figure of merit (53.6−1.6 Å)	SHARP, 0.758 (0.458)		SOLOMON, 0.915 (0.860)
phasing power$_{acentric}$ (iso/ano)	(λ1) 1.49/2.67	(λ2) 3.66/3.04	(λ3) 3.07/1.39

Refinement					
	R_{cryst} (%)	R_{free} (%)	Δ_{bonds} (Å)	Δ_{angles} (deg)	Ramachandran analysis
seleno-Met CT-1 (1.6 Å)	18.2	24.2	0.010	2.13	93.1 (6.9)
native CT-2 (1.7 Å)	20.7	28.0	0.011	2.18	89.6 (10.4)

[a] R_{merge} gives the average agreement between the independently measured intensities. $\langle I/\sigma(I)\rangle$ is the root-mean-square value of the intensity measurements divided by their estimated standard deviation. The values for the highest-resolution shells are given in parentheses. R_{cryst} is the crystallographic residual following refinement. R_{free} is the cross-validated R factor calculated with 10% of the data omitted from refinement. Δ_{bonds} and Δ_{angles} give the average departure from ideal values of the bond lengths and angles, respectively. Values for the Ramachandran analysis indicate the percentage of residues exhibiting main chain dihedral angles found in the most favored and additionally allowed regions.

for Gly[216] and Tyr[217]. The model was built using O (*27*) and refined with TNT (*28*). The structure of the CT-2 variant was determined by using residues 27−206 of the CT-1 model as the search model in AMORE (*29*). Careful rebuilding of the model revealed residues 29−228, though the density for residues 29−43 was significantly weaker than in the CT-1 structure.

RESULTS AND DISCUSSION

MsrA Architecture. The structure of bMsrA is of the mixed α/β type, with secondary structure elements in the sequence β1, α1, β2, α2, β3, α3, β4, β5, β6, α4, β7, β8, and α5 (Figure 1A). A search with DALI (*31*) showed that the core region (β1, α1, β2, β3, and α3) has topology corresponding to the two-layer sandwich, $\alpha-\beta$ plaits motif. For example, 109 α-carbon atoms can be superimposed on a subdomain of formiminotransferase cyclodeaminase (*32*) with root-mean-square agreement of 4.0 Å. The level of sequence identity is low (13%), however, not indicative of divergent evolution. This core of bMsrA is elaborated by extending the antiparallel β-sheet to a six-stranded, mixed β-sheet. The "Gly[71]-Cys-Phe-Trp-Gly[75]" motif (Figure 1B), which defines the location of the presumed active site, is at the apex of α1 and β1 (Figure 1A). In addition, α2 and a small, two-stranded sheet (β4 and β5) contribute residues to this region. In the first crystal modification (CT-1, Table 1), the electron density (Figure 1B) displayed the fortuitous trapping of a covalent DTT complex with Cys[72] and Cys[218]. The S$^{\gamma}$ atom of Cys[72] is located at the N-terminus of α1 near the helical axis (Figure 1C). A water molecule bridges the DTT molecule and Tyr[103], Glu[115], and Tyr[155].

The second modification of the protein, CT-2, includes 10 additional residues (Leu[220]−Leu[229]) at the C-terminus. In the context of this extended "tail", and lacking the interaction with DTT, Cys[218] adopts a different conformation (Figure 1D). The tail itself, which is glycine-rich, is rather extended and makes limited contacts to the rest of the protein. In this crystal form, a surface loop (residues 163−166) from a symmetry-related molecule also binds near the active site (Figure 2A). This crystal contact is chiefly via water-mediated hydrogen bonds, although direct interactions were found from the amide nitrogen atom of Ala[164] and the side chain of Glu[165] to Asp[150] and Tyr[155], respectively. This contact suggests how the surface-exposed active site could

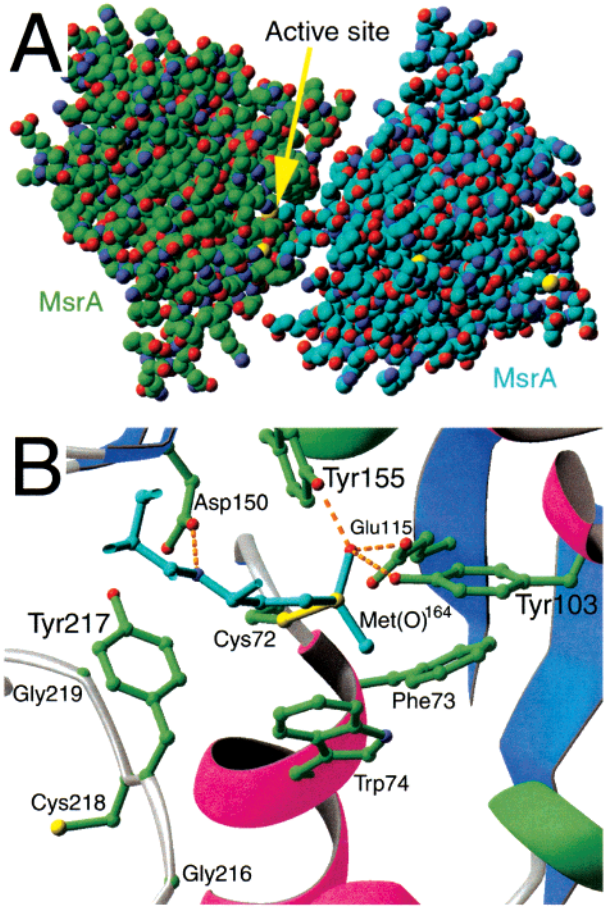

FIGURE 2: (A) Space-filling representation of the contact between the surface loop of residues Ser[163]−His[166] of one molecule of MsrA and the active site of the neighboring molecule of MsrA within the CT-2 crystals. (B) Putative model for the transition-state intermediate. The loop containing the Met-*S*-(O)[164] model (cyan) has been truncated for clarity. Dashed, gold bonds represent potential hydrogen bonding interactions.

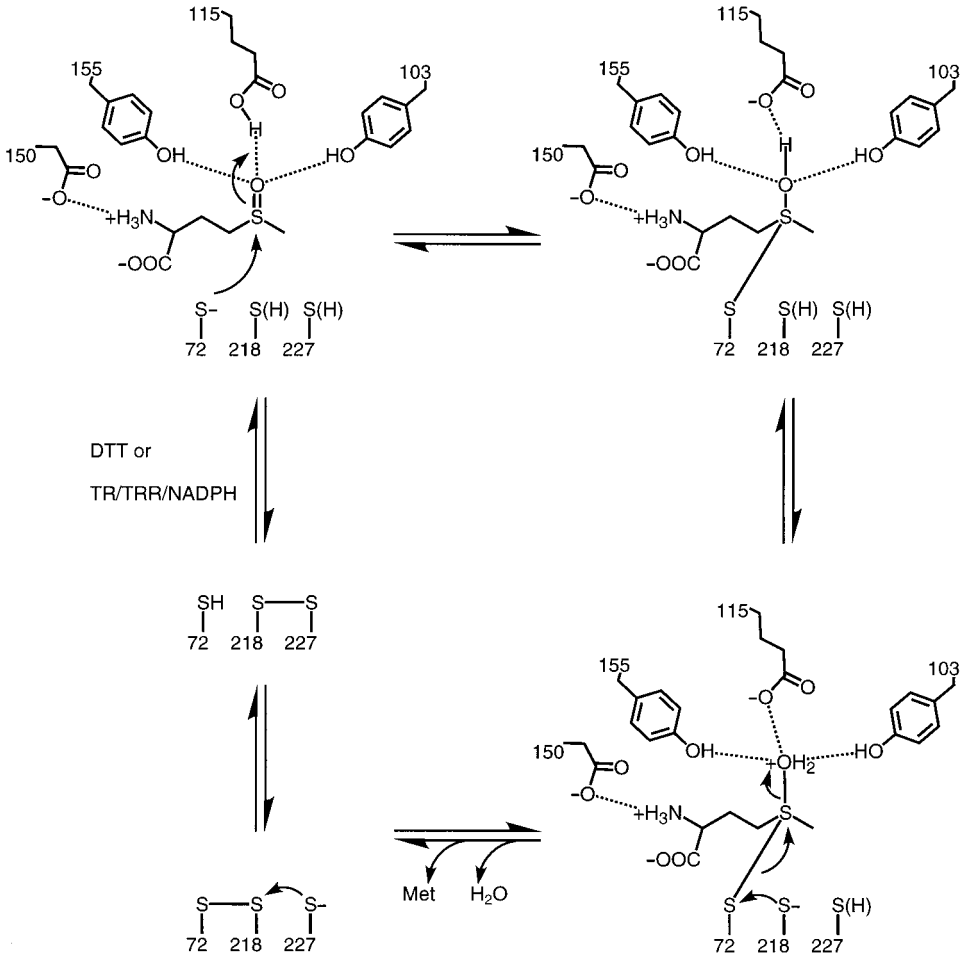

FIGURE 3: Proposed reaction mechanism for bMsrA. The residues that are shown are thought to provide interactions that facilitate the binding and activation of substrate and the stabilization and breakdown of the covalent intermediate. Breakdown of the intermediate can occur via intra- or intermolecular thiol−disulfide exchange (see the text). For class I MsrAs (see the text), including bMsrA and hMsrA, this process is most likely mediated through Cys residues (Cys^{218} and Cys^{227}) within a glycine-rich C-terminal tail that shuttles electrons from the thioredoxin−thioredoxin reductase system (TR and TRR, respectively). Class II MsrAs may alternatively utilize either thioredoxin or their own cysteine-containing, C-terminal domains to return the active site to the fully reduced state for another round of catalysis.

freely interact with small peptides and macromolecular protein substrates, as well as its in vivo thio−disulfide exchange partner, thioredoxin. Despite having part of another bMsrA molecule within the active site, the C-terminal tail appears to be unhindered (Figure 2B) and can still access Cys^{72}.

Putative Transition State. On the basis of the CT-2 crystal contact and the CT-1−DTT complex, a model of a covalent, trigonal-bipyramidal, reaction intermediate was generated (Figure 2B). The side chain of Ala^{164} was extended and modified to resemble Met-*S*-(O). Only minor adjustments to the side chains of Cys^{72}, Tyr^{103}, and the $Met(O)^{164}$ analogue were needed to establish reasonable interactions with Tyr^{103}, Glu^{115}, and Tyr^{155}. The backbone hydrogen bond to Asp^{150} was retained, representing a potential binding interaction with the amino nitrogen atom of free Met or the backbone amide linkage of polypeptide substrates.

The putative transition-state binding mode provides a rationale for the observed substrate specificity of MsrAs and the effects of mutations on activity. Consistent with its central role, mutation of Cys^{72} completely inactivates the enzyme (*12*, *19*). The terminal ϵ-methyl group of Met(O) binds in a shallow pocket generated by Phe^{73} and Trp^{74} (Figure 2B). Consistent with the known specificity of the enzyme, the bulky nature of these side chains precludes the binding of substrates larger than methionine (*11*). The mutation of these residues also leads to complete inactivation (*19*). The model for the transition state is compatible with the observation that MsrAs are only able to reduce the *S*-form of the sulfoxide moiety (*19*, *20*). The possibility that the reaction mechanism may occur through a sulfenic acid intermediate (*19*) was examined by trying to dock the intermediate so that nucleophilic attack would occur at the oxygen atom of the sulfoxide (*33*). A plausible orientation was not, however, immediately apparent.

Reaction Mechanism. A reaction scheme (Figure 3) was formulated using a combination of the available data and the historical literature on small molecule reactions of thiols with sulfoxides (*34*−*36*). The proposed scheme involves the overall transfer of two protons and two electrons and appears to be unique among other known reductases (*12*, *33*, *37*−*39*). Cys^{72} is activated and stabilized as the thiolate anion due to its location at the positive end of the α1 helix dipole (Figure 1C). Studies on thioredoxin and model peptides suggest that this favorable interaction could decrease the thiol pK_a from ~8.8 by several pH units (*40*). Attack on the sulfur atom of Met(O) by Cys^{72} may also be encouraged by simultaneous proton transfer from Glu^{115}. The resulting

tetravalent sulfur intermediate is stabilized by interactions with Tyr^{103}, Glu^{115}, and Tyr^{155} (Figure 2B). A subsequent proton-transfer step and the attack of Cys^{218} on Cys^{72} facilitate the loss of water and collapse of the intermediate to the sulfide of methionine. The active site is returned to a fully reduced state by thiol−disulfide exchange via Cys^{227} and either DTT or a thioredoxin-regeneration system.

The structure supports the prior suggestion (*12*) that three thiols (Cys^{72}, Cys^{218}, and Cys^{227}) participate in catalysis. The first two are directly in the active site, and the third can move closer via movement of the glycine-rich C-terminal tail (Figure 1). Support for the direct involvement of Cys^{218} and Cys^{227} in the reaction mechanism comes from the mass spectrometric determination of the free sulfhydryl states of all Cys mutant pairs of bMsrA (*12*). Only upon treatment with substrate was a disulfide bond formed between either Cys^{72} and Cys^{218} or Cys^{72} and Cys^{227}. The inability of DTT to restore the activity of the Cys^{218} variants, in contrast to the Cys^{227} mutants, also suggests that Cys^{218} is the preferred thiol for the release of product (*12*). Moreover, the observed increase in enzyme activity with DTT, as compared to thioredoxin for the Cys^{227} variants, indicates that the role of Cys^{227} is to facilitate the transfer of electrons from thioredoxin. These observations support the possibility that the C-terminal tail can flip in and out of the active site (Figures 1D and 2B). It is also clear that if, for example, Cys^{218} is removed, a thiol group in the vicinity can compensate and restore activity. This thiol can be either from the protein, i.e., Cys227, or from an exogenous source, i.e., DTT or thioredoxin.

C-Termini Comparisons. A comparison of 20 putative and known MsrA domains shows that there is some diversity in the location and number of Cys residues at the C-termini (*12*). The observation that the thiol needed for the release of the product can come from a variety of intra- and intermolecular sources may account for the variation seen in this region. Nonetheless, these differences raise the question of whether the role for the C-terminal tail in the reaction mechanism proposed for bMsrA is applicable to the entire family. Closer inspection of the alignment suggests that bMsrA and hMsrA belong to a subclass of MsrAs characterized by a glycine-rich, C-terminal tail that contains one or two Cys residues. We refer to this subclass as "type I". In contrast, the "type II" MsrAs are characterized by a highly conserved C-terminal extension (∼17 kDa) of unknown function. Both classes of MsrAs contain a Cys residue at or near Cys^{218}. Those MsrAs that do not contain a Cys^{227} equivalent most probably rely on thioredoxin for reducing the disulfide bond formed between Cys^{72} and Cys^{218}. It is tempting to speculate that the C-terminal domain of the type II enzymes, which contains two Cys residues, may modulate activity. Two outliers in this analysis are the MsrAs from *Drosophila melanogaster* and *Bacillus subtilis*. The former enzyme is only slightly homologous to either the type I or type II MsrAs at the C-terminus. Interestingly, the *B. subtilis* enzyme has a Cys residue equivalent to Gly^{75} in bMsrA. Molecular modeling suggests that this residue could enable catalysis by the formation of a disulfide bond in a manner similar to that of the CysXXCys motif seen in the thioredoxin family (*40*).

Summary. The key players in MsrA catalysis are seen to be Cys^{72}, Phe^{73}, and Trp^{74} of the Gly-Cys-Phe-Trp-Gly motif, the residues that bind the oxygen atom of the sulfoxide moiety, Tyr^{103}, Glu^{115}, and Tyr^{155}, and possibly the substrate contact residue Asp^{150}. In 19 out of 20 MsrA sequences, all of these residues are conserved, and in the 20th, only Tyr^{203} and Asp^{150} are changed. This remarkable conservation emphasizes the importance of Met(O) reduction by MsrA in all organisms.

ACKNOWLEDGMENT

We gratefully acknowledge the technical assistance of L. S. Gay, M. Wang, D. A. McMillen, and Y. Wang. We thank W. A. Breyer and Dr. A. M. Orville for help with crystallographic computing programs and data collection. We thank Drs. J. Honek and M. Quillin for their insightful discussions and comments on the manuscript. This work is based in part upon data collected at the Stanford Synchrotron Radiation Laboratory (SSRL) which is funded by the Department of Energy and the National Institutes of Health.

NOTE ADDED IN PROOF

A recent report suggests that the transition state intermediate proposed herein can collapse in an alternative manner to form a sulfenic intermediate on Cys^{72} (*41*). All other aspects of the proposed mechanism are supported.

REFERENCES

1. Stadtman, E. R., and Berlett, B. S. (1998) *Drug Metab. Rev. 30*, 225.
2. Squier, T. C., and Bigelow, D. J. (2000) *Front. Biosci. 5*, D504.
3. Vogt, W. (1995) *Free Radical Biol. Med. 18*, 93.
4. Grune, T., and Davies, K. J. (1997) *Biofactors 6*, 165.
5. Levine, R. L., Berlett, B. S., Moskovitz, J., Mosoni, L., and Stadtman, E. R. (1999) *Mech. Ageing Dev. 107*, 323.
6. Ciorba, M. A., Heinemann, S. H., Weissbach, H., Brot, N., and Hoshi, T. (1997) *Proc. Natl. Acad. Sci. U.S.A. 94*, 9932.
7. Chen, J., Avdonin, V., Ciorba, M. A., Heinemann, S. H., and Hoshi, T. (2000) *Biophys. J. 78*, 174.
8. Mushegian, A. R., and Koonin, E. V. (1996) *Proc. Natl. Acad. Sci. U.S.A. 93*, 10268.
9. Moskovitz, J., Jenkins, N. A., Gilbert, D. J., Copeland, N. G., Jursky, F., Weissbach, H., and Brot, N. (1996) *Proc. Natl. Acad. Sci. U.S.A. 93*, 3205.
10. Kuschel, L., Hansel, A., Schonherr, R., Weissbach, H., Brot, N., Hoshi, T., and Heinemann, S. H. (1999) *FEBS Lett. 456*, 17.
11. Moskovitz, J., Weissbach, H., and Brot, N. (1996) *Proc. Natl. Acad. Sci. U.S.A. 93*, 2095.
12. Lowther, W. T., Brot, N., Weissbach, H., Honek, J. F., and Matthews, B. W. (2000) *Proc. Natl. Acad. Sci. U.S.A. 97*, 6463.
13. Moskovitz, J., Berlett, B. S., Poston, J. M., and Stadtman, E. R. (1997) *Proc. Natl. Acad. Sci. U.S.A. 94*, 9585.
14. Moskovitz, J., Rahman, M. A., Strassman, J., Yancey, S. O., Kushner, S. R., Brot, N., and Weissbach, H. (1995) *J. Bacteriol. 177*, 502.
15. Wizemann, T. M., Moskovitz, J., Pearce, B. J., Cundell, D., Arvidson, C. G., So, M., Weissbach, H., Brot, N., and Masure, H. R. (1996) *Proc. Natl. Acad. Sci. U.S.A. 93*, 7985.
16. Hassouni, M. E., Chambost, J. P., Expert, D., Van Gijsegem, F., and Barras, F. (1999) *Proc. Natl. Acad. Sci. U.S.A. 96*, 887.
17. Vriesema, A. J., Dankert, J., and Zaat, S. A. (2000) *Infect. Immun. 68*, 1061.
18. Gabbita, S. P., Aksenov, M. Y., Lovell, M. A., and Markesbery, W. R. (1999) *J. Neurochem. 73*, 1660.
19. Moskovitz, J., Poston, J. M., Berlett, B. S., Nosworthy, N. J., Szczepanowski, R., and Stadtman, E. R. (2000) *J. Biol. Chem. 275*, 14167.

20. Sharov, V. S., Ferrington, D. A., Squier, T. C., and Schöneich, C. (1999) *FEBS Lett. 455*, 247.
21. Brot, N., Weissbach, L., Werth, J., and Weissbach, H. (1981) *Proc. Natl. Acad. Sci. U.S.A. 78*, 2155.
22. Gassner, N. C. (1998) Ph.D. Thesis, University of Oregon, Eugene, OR.
23. Otwinowski, Z., and Minor, W. (1997) *Methods Enzymol. 276*, 307.
24. Terwilliger, T. C., and Berendzen, J. (1999) *Acta Crystallogr. D55*, 849.
25. de La Fortelle, E., and Bricogne, G. (1997) *Methods Enzymol. 276*, 472.
26. Abrahams, J. P., and Leslie, A. G. (1996) *Acta Crystallogr. D52*, 30.
27. Jones, T. A., Zou, J. Y., Cowan, S. W., and Kjeldgaard, M. (1991) *Acta Crystallogr. A47*, 110.
28. Tronrud, D. E. (1997) *Methods Enzymol. 277*, 306.
29. Navaza, J. (1994) *Acta Crystallogr. A50*, 157.
30. Carson, M. (1997) *Methods Enzymol. 277*, 493.
31. Holm, L., and Sander, C. (1995) *Trends Biochem. Sci. 20*, 478.
32. Kohls, D., Sulea, T., Purisima, E. O., MacKensie, R. E., and Vrielink, A. (2000) *Structure 8*, 35.
33. Claiborne, A., Yeh, J. I., Mallet, T. C., Luba, J., Crane, E. J., III, Charrier, V., and Parsonage, D. (1999) *Biochemistry 38*, 15407.
34. Wallace, T. J., and Mahon, J. J. (1965) *J. Org. Chem. 30*, 1502.
35. Wallace, T. J. (1964) *J. Am. Chem. Soc. 86*, 2018.
36. Wallace, T. J., and Mahon, J. J. (1964) *J. Am. Chem. Soc. 86*, 4099.
37. Stubbe, J., and van der Donk, W. A. (1998) *Chem. Rev. 98*, 705.
38. Pollock, V. V., and Barber, M. J. (1997) *J. Biol. Chem. 272*, 3355.
39. Schindelin, H., Kisker, C., Hilton, J., Rajagopalan, K. V., and Rees, D. C. (1996) *Science 272*, 1615.
40. Kortemme, T., and Creighton, T. E. (1995) *J. Mol. Biol. 253*, 799.
41. Boschi-Muller, S., Azza, S., Sanglier-Cianferani, S., Talfournier, F., Van Dorsselear, A., and Branlant, G. (2000) *J. Biol. Chem.* (in press).

BI0020269